Radiology

Pontine Infarction: Diffusion-Tensor Imaging of Motor Pathways—A Longitudinal Study[1]

Miao Zhang, MD
Qixiang Lin, PhD
Jie Lu, MD, PhD
Dongdong Rong, MD
Zhilian Zhao, MD
Qingfeng Ma, MD
Hesheng Liu, PhD
Ni Shu, PhD
Yong He, PhD
Kuncheng Li, MD, PhD

Purpose: To investigate the dynamic evolution of diffusion indexes in the corticospinal tract (CST) distal to a pontine infarct by using diffusion-tensor imaging, to determine the relationship of these indexes with clinical prognosis, and to explore the structural changes in the motor pathway during recovery.

Materials and Methods: This study was approved by the institutional ethics committee, and written informed consent was obtained from each participant. Seventeen patients with pontine infarct underwent five diffusion-tensor imaging examinations during a period of 6 months (within 7 days of onset, 14, 30, 90, and 180 after onset). Fractional anisotropic values were measured in the medulla, cerebral peduncle, internal capsule, and centrum semiovale. Fractional anisotropic values of the CST in the ipsilateral side of the infarct were compared with those in the contralateral sides and those in control subjects by using the Student t test and one-way analysis of variance, and their relationships with clinical scores were analyzed by using Pearson correlation analysis. Reconstructions of the CST were performed. Structural changes of the damaged CST were followed up.

Results: Fractional anisotropic ratios in the CST above the pons decreased significantly compared with those in the contralateral side and those in control subjects within 7 days, on day 14, and on day 30 after onset ($P < .001$). Fractional anisotropic ratios above the pons on day 14 correlated positively with Fugl-Meyer scores on day 90 ($r = 0.771$, $P < .001$) and day 180 ($r = 0.730$, $P = .001$). Follow-up diffusion-tensor tractographic images showed regeneration and reorganization of the motor pathways.

Conclusion: Secondary degeneration of the CST can be detected at diffusion-tensor imaging in the early stages after pontine infarction, which could help predict the motor outcomes. Diffusion-tensor tractography can allow detection of regeneration and reorganization of the motor pathways during recovery.

© RSNA, 2014

© RSNA, 2014

Because impairment of motor function is one of the most seriously disabling sequelae of ischemic stroke, authors of many studies (1–4) have attempted to elucidate the motor recovery mechanisms after infarction. Diffusion-tensor (DT) imaging, a noninvasive magnetic resonance (MR) imaging technique, allows measurement of the random motion of water molecules and provides information about cellular integrity and pathology. In a highly ordered white matter tract, water molecules diffuse faster in the direction parallel to the tract than in the perpendicular direction, because axonal membranes and myelin sheaths restrict transverse diffusion. Pathologic processes that change the microstructural environment, such as neuronal size, extracellular space, and tissue integrity, result in altered diffusion. Molecular diffusion can be measured with several indexes derived from DT

imaging data. DT imaging is advantageous for identification and estimation of neural tracts at the subcortical level (5,6). Furthermore, the new technique of DT tractography allows the visualization of the integrity of the corticospinal tract (CST), which is the major neuronal pathway that mediates voluntary movements and is the most important motor pathway for predicting motor outcome in the human brain.

For the past decade, great contributions to research on the mechanisms of motor recovery after stroke were made with DT imaging. However, most previous DT imaging studies were focused on patients who experienced infarction of the middle cerebral artery (7–11), but little is known about the motor recovery mechanisms in patients with pontine infarction. Compared with supratentorial cerebral infarction, the spatial relationship between the pontine infarct lesion and the fiber tract is more complex, and its effect on patient outcome is poorly understood. Furthermore, few longitudinal studies of motor recovery mechanisms in patients with pontine infarct have been reported (12,13). Thus, in the present study, we used DT imaging to investigate *(a)* the dynamic evolution of the diffusion indexes in the CST distal to the pontine infarct, *(b)* the relationship between diffusion indexes of the CST on the ipsilateral side of the infarct in the early stages after infarction and clinical prognosis; and *(c)* the structural changes of the motor pathway during stroke recovery.

Materials and Methods

Subjects

This prospective study was approved by the institutional review board. Each subject provided written informed consent.

A total of 17 subjects were included in the study from December 2008 to February 2012. The criteria for enrollment were *(a)* admission within 7 days of the onset of symptoms and availability of complete patient history, *(b)* a single infarct confined to the pons identified at MR imaging, *(c)* no other neurologic or psychiatric disorders, and *(d)* no other concomitant brain lesion or previous infarcts shown at conventional MR imaging. The exclusion criteria were *(a)* contraindications for MR imaging, *(b)* unclear onset of symptoms, *(c)* lesions outside the pons or extensive infarcts involving the midbrain or the medulla, *(d)* recurrence infarction or secondary hemorrhage during follow-up, *(e)* deafness and/or blindness, aphasia, or a visual field deficit, and *(f)* patient inability to complete follow-up examination. Of 30 patients recruited according to the inclusion criteria, 13 were excluded on the basis of the exclusion criteria. One patient was excluded owing to contraindications for MR imaging, three patients were excluded for a larger infarct that exceeded the midline of the pons, two patients were excluded for recurrence infarction during follow-up, one patient was excluded for aphasia, and

Advances in Knowledge

- Diffusion-tensor imaging can help detect the reduction in fractional anisotropic values of the corticospinal tract (CST) distal to the pontine infarct in the early stage after the infarction.

- Fractional anisotropic ratios in the CST above the infarct on day 14 correlated positively with Fugl-Meyer scores on day 90 ($r = 0.771$, $P < .001$) and day 180 ($r = 0.730$, $P = .001$).

- Contrary to the results of most previous studies on middle cerebral artery infarction, secondary degeneration of the CST after pontine infarction was found to be relatively mild and recoverable and associated with the size and location of the infarct occurred.

- Patient follow-up revealed evidence of structural remodeling and motor pathway compensation, providing an important basis for studies examining the recovery of motor function after pontine infarction.

Implication for Patient Care

- The results of this study have important implications for the motor recovery mechanism and rehabilitation of patients with pontine infarction.
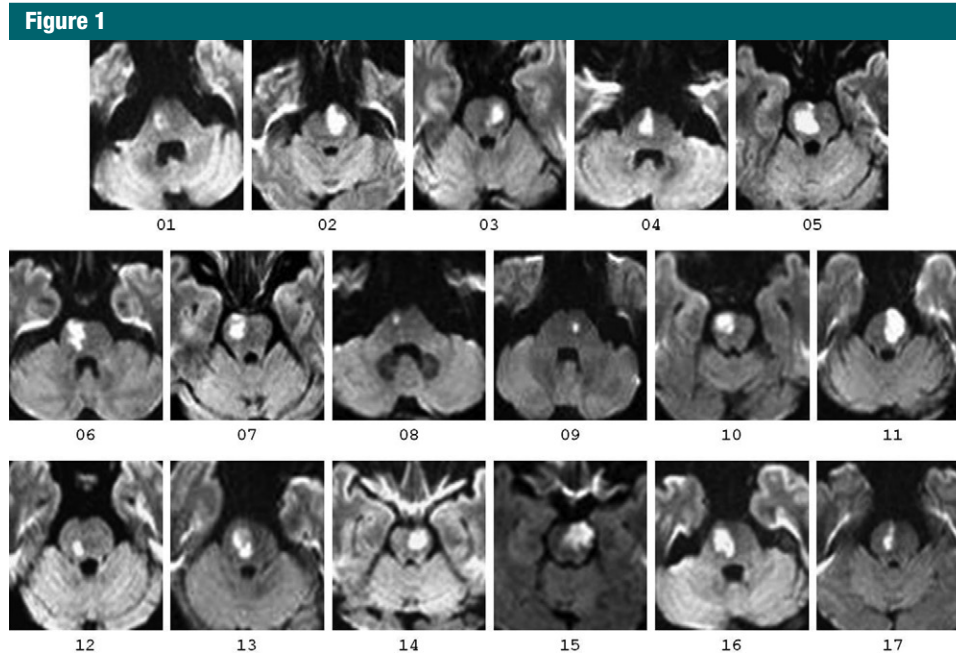
Radiology

Figure 1

Figure 1: Axial diffusion-weighted images illustrate pontine lesion locations. Numbers below images correspond to patient numbers in Table 1.

another six patients were unable to complete the follow-up examinations for personal reasons. The remaining 17 patients (12 men, five women; mean age, 58.3 years; range, 34–73 years) were included in our analyses. Eleven subjects had pontine infarctions on the right side, and six had infarctions on the left side of the CST. The volumes of the pontine infarct lesions were measured at diffusion-weighted imaging during the first visit. The volumes of the infarctions ranged from 2.6 mL to 29.7 mL (mean, 15.0 mL). Diagnosis and volume measurement of the infarcts were performed by radiologists (M.Z. and D.D.R., with 14 and 11 years of experience in neuroimaging, respectively). The locations of the infarcts are shown in Figure 1. All patients had first-onset stroke and presented with motor deficits. All patients were imaged five times during a period of 6 months (within 7 days and 14, 30, 90, and 180 days after stroke onset). The demographic and clinical characteristics of patients are summarized in Table 1. Seventeen healthy control subjects who were matched according to patient age, sex, and handedness were

recruited and imaged five times in 6 months (the intervals between examinations were 15 days in the 1st month, then 90 and 180 days).

MR Imaging Protocol

We examined all subjects with a 3.0-T MR imager (Magnetom Trio Tim; Siemens, Erlangen, Germany) equipped with gradient hardware allowing up to 23 mT/m. Traditional axial T1-weighted, fast spin-echo T2-weighted, fluid attenuation inversion-recovery, and diffusion-weighted imaging examinations were performed. Consecutive images of sections were acquired in an identical location for all sequences, with a 5-mm section thickness. The acquisition parameters for the T1-weighted sequence were repetition time msec/echo time msec of 155/2.81 and imaging time of 50 seconds; for the fast spin-echo T2-weighted sequence, 3830/98 and imaging time of 51 seconds; for the fluid attenuation inversion-recovery sequence, 8500/87 and imaging time of 1 minute 44 seconds; and for the diffusion-weighted imaging sequence, 3000/91 with b values of 0, 500, and 1000 sec/mm^2 and

imaging time of 1 minute 14 seconds. For DT imaging, an echo-planar imaging sequence was used with 8000/83; number of signals acquired, one; matrix, 128×128; field of view, 24×24 cm; b values of 0 and 700 sec/mm^2; and section thickness, 2 mm without a gap. We used a parallel acquisition technique with an acceleration factor of two to reduce the acquisition time and allow us to obtain images with less distortion from susceptibility artifacts. In addition, diffusion-sensitive gradients were applied along 64 gradient directions. The imaging baseline was parallel to the anterior commissure-to-posterior commissure line to keep the central sections of the last four sequences consistent with that of the first sequence, and a standard head coil was used. The DT imaging acquisition time was 9 minutes 6 seconds.

DT imaging Data Postprocessing

Image preprocessing was performed by two MR imaging researchers (Q.L. and N.S., with 3 and 10 years of experience in MR research, respectively). DT imaging data were transferred to a computer workstation with a Windows

Table 1

Patient Demographic and Clinical Characteristics

Patient No.	Age (y)	Sex	Symptoms	Pontine Infarct on Diffusion-weighted Image		
				Side	Volume (mL)	Location
01	57	M	Left hemiparesis	Right	6.0	Right ventromedial lower pons
02	59	M	Right hemiparesis, dysarthria	Left	18.4	Left ventromedial midpons
03	48	M	Right hemiparesis, dysarthria	Left	11.9	Left ventromedial midpons
04	63	M	Left pure motor hemiparesis	Right	14.2	Right ventromedial lower pons
05	60	M	Left hemiparesis, dizziness	Right	27.1	Right ventromedial upper pons
06	61	M	Left hemiparesis, dysarthria	Right	18.0	Right ventromedial lower pons
07	56	M	Left hemiparesis	Right	15.9	Right ventrolateral midpons
08	68	M	Left pure motor hemiparesis, dizziness	Right	2.6	Right ventrolateral lower pons
09	62	M	Right hemiparesis, dizziness	Left	3.8	Left ventromedial lower pons
10	73	F	Left hemiparesis, dizziness	Right	15.5	Right ventrolateral lower pons
11	34	F	Right hemiparesis, dysarthria	Left	29.7	Left ventromedial midpons
12	56	M	Left hemiparesis	Right	9.6	Right ventrolateral midpons
13	54	M	Left hemiparesis, dysarthria, dizziness	Right	14.6	Right ventromedial midpons
14	60	M	Right hemiparesis, dysarthria, dizziness	Left	18.7	Left ventromedial upper pons
15	62	F	Right hemiparesis, dizziness	Left	20.0	Left ventromedial upper pons
16	64	F	Left hemiparesis, dizziness	Right	22.7	Right ventromedial midpons
17	54	F	Left hemiparesis, dizziness	Right	6.1	Right ventrolateral upper pons

platform and processed by using DT imaging studio analysis software. All preprocessing procedures were implemented by using free software (FSL; Oxford Centre for Functional MR Imaging of the Brain, Oxford, England). For every examination of each subject, the diffusion-weighted images were registered to the corresponding images with b values of 0 sec/mm^2 and an affine transformation to correct for eddy-current distortion and head motion. To follow DT imaging metrics in the same regions of interest (ROIs), we coregistered the DT images from all time points before measurement. For each subject, each of the follow-up images with a b value of 0 sec/mm^2 was aligned to the corresponding image with a b value of 0 sec/mm^2 at the first time point by using affine transformation, and the derived transformation matrix was then applied to the corresponding parametric maps. DT imaging data were interpolated into $1 \times 1 \times 1$–mm voxels. The DT of each voxel was calculated by using a linear least squares fitting algorithm. After diagonalization of the DT, the DT eigenvalues (λ_1, λ_2, and λ_3) were obtained and the λ_{2-3} was generated

Figure 2

Figure 2: Illustration of brain shows ROIs (blue circles) of the CST.

by averaging λ_2 and λ_3. The fractional anistropic (FA) value was derived for each voxel according to the following equation:

$$FA = \sqrt{\frac{(\lambda_1 - \lambda_2)^2 + (\lambda_1 - \lambda_3)^2 + (\lambda_2 - \lambda_3)^2}{2(\lambda_1 + \lambda_2 + \lambda_3)^2}}.$$

Referring to anatomic knowledge and MR imaging baseline results, we placed ROIs symmetrically on images of the axial sections in the left and right sides along the pyramidal tract pathway at four levels: the medulla, cerebral peduncle, internal capsule, and centrum semiovale (Fig 2). The ROIs were
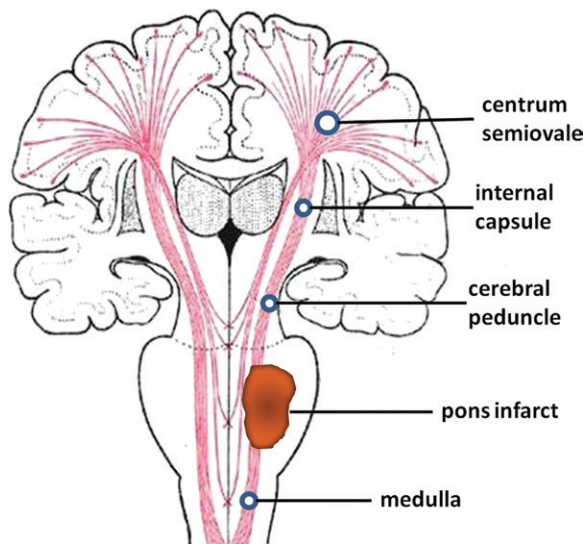
Radiology

Table 2

FA Values of the Infarct Side and Contralateral Side at Five Time Points

ROI	Patient Group (n = 17)					Control Group (n = 17)
	<7 Days	14 Days	30 Days	90 Days	180 Days	
Centrum semiovale						0.48 ± 0.03
Infarct side	0.44 ± 0.05*	0.42 ± 0.04*	0.44 ± 0.06*	0.43 ± 0.07	0.45 ± 0.06	...
Contralateral side	0.47 ± 0.05	0.47 ± 0.04	0.48 ± 0.07	0.46 ± 0.04	0.46 ± 0.04	...
Internal capsule						0.64 ± 0.04
Infarct side	0.59 ± 0.09*	0.57 ± 0.05*†	0.60 ± 0.07*	0.62 ± 0.06	0.63 ± 0.06	...
Contralateral side	0.64 ± 0.07	0.64 ± 0.07	0.65 ± 0.04	0.63 ± 0.08	0.64 ± 0.07	...
Cerebral peduncle						0.72 ± 0.04
Infarct side	0.63 ± 0.12*†	0.62 ± 0.12*†	0.65 ± 0.10*	0.67 ± 0.09	0.70 ± 0.09	...
Contralateral side	0.71 ± 0.06	0.73 ± 0.11	0.71 ± 0.08	0.71 ± 0.08	0.71 ± 0.13	...
Above the pons‡						0.62 ± 0.02
Infarct side	0.56 ± 0.06*†	0.54 ± 0.04*†	0.56 ± 0.04*†	0.57 ± 0.03*†	0.59 ± 0.05	...
Contralateral side	0.61 ± 0.04	0.61 ± 0.05	0.62 ± 0.04	0.60 ± 0.04	0.60 ± 0.05	...
Medulla						0.34 ± 0.05
Infarct side	0.34 ± 0.15	0.29 ± 0.08*	0.27 ± 0.07*	0.28 ± 0.11*	0.27 ± 0.07*	...
Contralateral side	0.35 ± 0.08	0.36 ± 0.11	0.35 ± 0.11	0.35 ± 0.09	0.32 ± 0.10	...

Note.—Data are means ± standard deviation.

* Significantly different from contralateral side, $P < .05$.

† Significantly different from control subjects, $P < .05$.

‡ Above the pons includes the cerebral peduncle, internal capsule, and centrum semiovale.

automatically defined as a circle with an area of 30–45 mm^2 depending on the size of the brain structure. The 45-mm^2 ROIs were placed at the midpoint of the anterior two-thirds of the centrum semiovale. The 35-mm^2 ROIs were placed in the middle of the posterior limb at the internal capsule and in the anterior part of the cerebral peduncle. At the medulla, the 30-mm^2 ROIs were placed ventrally. The ROI size was 25–30 voxels. Values for each ROI were obtained by averaging all voxels in the ROI. The FA ratio (rFA) between the ipsilateral side of the infarct (FA$_{ips}$) and contralateral side (FA$_{con}$) was calculated as rFA = FA$_{ips}$/FA$_{con}$ in each patient.

DT imaging data were then transferred to a workstation (Multi-Modality Work Place; Siemens) for further processing. The three-dimensional CST was reconstructed by a radiologist (M.Z., with 14 years of experience in neuroimaging) using software (Siemens). For fiber tracking of the CST, two ROIs were manually placed on two-dimensional transverse color-coded directional FA images. The upper ROI was placed on the posterior limb of the internal capsule, and the lower ROI was placed on the lower pons. Only the fibers passing through both ROIs were displayed and designated as the CST. The thresholds of the tracking termination were 0.2 for the FA and 45° for the angle between two contiguous eigenvectors. The three-dimensional fiber tracts were then superimposed on axial diffusion-weighted images and T2-weighted images. The total computational time per subject for DT image processing was approximately 20 minutes, including index measurement and fiber tracking of the CST.

Behavioral Studies

During each visit, behavioral assessments were independently performed (Q.M., with 15 years of experience and a nonauthor with 10 years of experience in neurology, respectively) before and after MR imaging. The two scores were averaged to provide an estimate. Motor function, balance, sensation, and joint function of the upper limbs were assessed by using the Fugl-Meyer (FM) scale, which includes 33 tasks. Patient ability to complete each task was rated

on a scale of 0–2 (0, subject was unable to perform the task; 1, subject could partially perform the task; and 2, subject was able to perform the task). The sum of the 33 scores was then normalized to a score between 0 and 100, where 100 represented good performance on all 33 tasks. The modified Rankin scale and the Barthel index scores also were measured to evaluate the patient's neurologic deficit, motor deficit, and independence.

Statistical Analysis

All values are presented as means ± standard deviation. Statistical analysis was performed by using software (SPSS 13.0 for Windows; SPSS, Chicago, Ill). We tested the side differences in the diffusion indexes of the CST in healthy control subjects by using a paired-sample t test, but found no significant differences ($P > .05$). Thus, the diffusion indexes of both sides were averaged for group comparison. The FA values were compared for the ipsilateral and contralateral sides of the infarct by using a paired-samples t test. The difference in FA values of the ROIs of the CST on the

Table 3

FA Ratios of the CST at the Five Time Points in Patients and Controls

ROI	Patient Group ($n = 17$)					Control Group ($n = 17$)	F Value	P Value
	<7 Days	14 Days	30 Days	90 Days	180 Days			
Centrum semiovale	0.95 ± 0.08	0.91 ± 0.06	0.93 ± 0.09	0.95 ± 0.15	0.99 ± 0.11	1.01 ± 0.08	2.461	.038
Internal capsule	0.93 ± 0.07*	0.90 ± 0.05*	0.92 ± 0.09*	0.98 ± 0.11	0.97 ± 0.05	1.02 ± 0.03	6.656	.000
Cerebral peduncle	0.89 ± 0.17	0.86 ± 0.21	0.92 ± 0.14	0.95 ± 0.15	1.02 ± 0.28	1.04 ± 0.08	2.564	.032
Above the pons†	0.92 ± 0.09*	0.88 ± 0.10*	0.92 ± 0.06*	0.96 ± 0.08	0.99 ± 0.10	1.01 ± 0.03	6.406	.000
Medulla	0.98 ± 0.37	0.83 ± 0.29	0.79 ± 0.23	0.85 ± 0.33	0.88 ± 0.21	1.03 ± 0.12	1.850	.111

Note.—Data are means ± standard deviation.

* Significantly different from control group, $P < .05$ (Dunnett test).

† Above the pons includes the cerebral peduncle, internal capsule, and centrum semiovale.

ipsilateral side of the infarct and those in control subjects was determined by means of one-way analysis of variance followed by the Dunnett test. We also examined the differences in the FA ratio between patients with infarcts and control subjects by using the same statistical methods. A Pearson correlation was performed on data from patients with infarcts to test for correlations between changes in the FA ratio of the ROIs of the CSTs at the first two time points and the clinical measures (including FM, modified Rankin scale, and Barthel index scores) after 6 months. A P value of .05 (two tailed) was considered to indicate a significant difference for all statistical procedures.

Results

Dynamic Changes in Diffusion Indexes in the CST Distal to the Pontine Infarction

We found no differences in FA values of the CST in healthy control subjects at the five time points ($P > .05$). Thus, the FA values at the first time point were used for group comparison. Table 2 shows the FA values of the ROI of the infarct on the ipsilateral and contralateral side of the CST at the five time points in patients and control subjects. Compared with those of the contralateral side, the FA values of the infarct side in the cerebral peduncle, internal capsule, and centrum semiovale within 7 days, on day 14, and day 30, and in the medulla
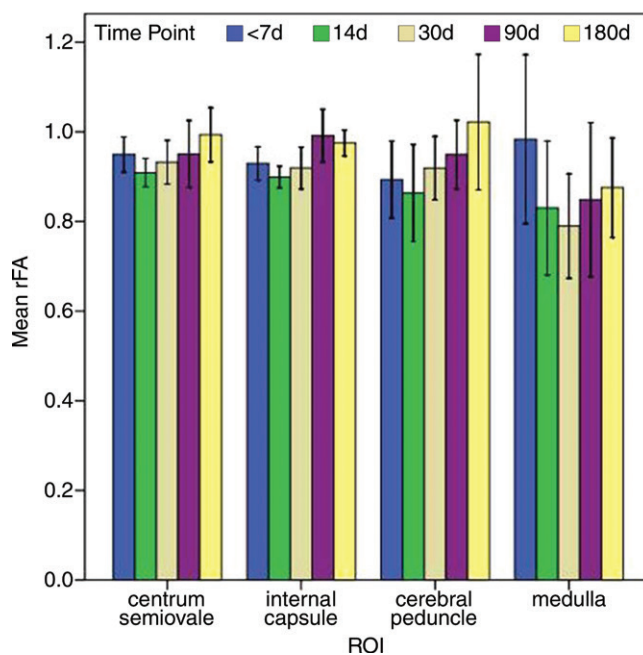
Figure 3

Figure 3: Bar graph shows dynamic changes in the FA ratio in the centrum semiovale, internal capsule, cerebral peduncle, and medulla, at different time points after stroke. d = days.

on days 14, 30, 90, and 180 were significantly lower ($P < .05$). Compared with those of the matched regions in control subjects, the FA values of the infarct side in the cerebral peduncle within 7 days ($P = .037$) and on day 14 ($P = .004$) and the internal capsule on day 14 ($P = .004$) were significantly lower. The FA values above the pons returned to normal on day 180, but the reduction in FA values in the medulla remained for a longer period of time, although the difference was not significant ($P > .05$). No obvious changes were found in control subjects and in matched regions located on the contralateral side in patients.

Table 3 shows the FA ratios (normalized FA values) in the medulla, cerebral peduncle, internal capsule, and

centrum semiovale at the five time points in patients and control subjects. Analysis of variance showed significant differences in the FA ratios in the cerebral peduncle ($F = 2.564$, $P = .032$), internal capsule ($F = 6.656$, $P < .001$), and centrum semiovale ($F = 2.461$, $P = .038$) compared with those in the control subjects. After post hoc (Dunnett) analyses, the FA ratios in the internal capsule within 7 days ($P = .004$), on day 14 ($P < .001$), and on day 30 ($P = .001$) after infarction were significantly lower compared with those in the control subjects. Figure 3 shows the dynamic changes in the FA ratio in the medulla, cerebral peduncle, internal capsule, and centrum semiovale with time after stroke.

Correlations between Early Changes in Diffusion Indexes and Clinical Outcomes

All patients had some degree of motor deficit. The FM scale scores ranged from 6 to 87 at the first examination. All patients received similar therapy for stroke. By the end of the 6th month, all patients had recovered somewhat; 11 patients returned to work, five were partially dependent, and two were completely dependent. The FM and Barthel index scores increased, and the modified Rankin scale scores decreased progressively with time. It was clinically important to test whether early changes in diffusion indexes of the degenerated CSTs could allow prediction of clinical outcomes in stroke patients. We found that the FA ratios above the pons on day 14 correlated positively with the FM scores on day 90 ($r = 0.771$, $P < .001$) and day 180 ($r = 0.730$, $P = .001$) and correlated negatively with the modified Rankin scale score on day 90 ($r = -0.569$, $P = .017$) and day 180 ($r = -0.498$, $P = .042$).

Pattern and Structural Remodeling of Ipsilateral CST Damage on DT Tractographic Images

The DT tractographic findings for our patients were classified into three grades according to the degree of CST involvement: grade 1 (five patients), integrity of the CST was preserved around the infarct, not compressed
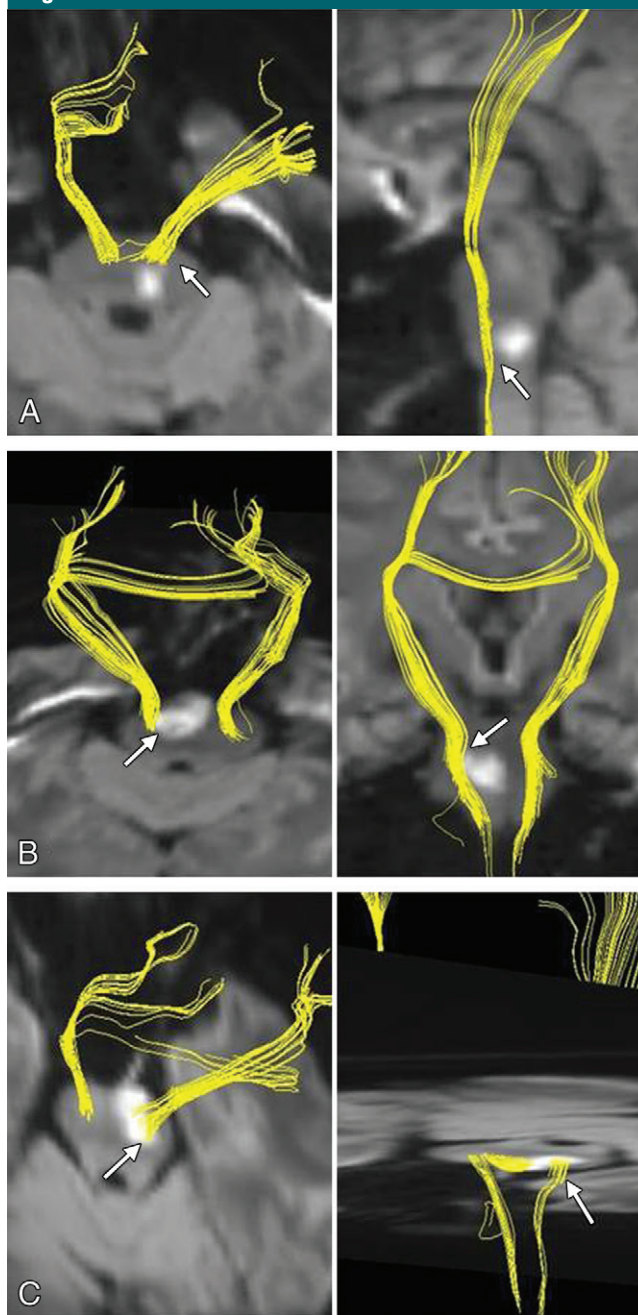

Figure 4

Figure 4: DT tractographic demonstration of three grades of findings classified according to the degree of CST involvement. *A*, Grade 1, with CST located in front of infarct and not compressed (arrows) on transverse (left) and sagittal (right) diffusion-weighted MR images; *B*, grade 2, CST compressed and curved (arrows) on transverse (left) and coronal (right) diffusion-weighted MR images; *C*, grade 3, CST mostly interrupted by infarct (arrows) on transverse diffusion-weighted MR images.

(Fig 4, *A*); grade 2 (three patients), the CST was compressed, curved, or slightly disrupted (Fig 4, *B*); grade 3 (nine patients), the CST was mostly or completely disrupted at the infarct (Fig 4, *C*). The grades according to CST

damage correlated negatively with FM ($r = -0.854$, $P < .001$) and Barthel index ($r = -0.770$, $P < .001$) scores at the first examination and correlated positively with the modified Rankin scale ($r = 0.789$, $P < .001$) score at the first examination.

Patients classified as grade 1 had normal findings shortly after onset of loss of function. The motor function of the patients with grade 2 CST involvement recovered gradually and returned to normal after 3 months. The patients found to have grade 3 CST involvement recovered slowly and had motor dysfunction after 6 months. Grades of CST damage correlated negatively with FM scores (r = -0.498, $P = .030$) on day 90, and did not correlate with Barthel index or modified Rankin scale scores on day 90. There was no significant correlation among the grades and FM, Barthel index, and modified Rankin scale scores on day 180. Figure 5 shows the changes in FM scores of patients with grades 1–3 CST involvement with time.

Follow-up DT tractographic imaging showed the dynamic changes of severely damaged CSTs during stroke recovery. The regeneration and functional reorganization of the motor pathway was detected in eight patients on days 90 and 180. In five of eight patients, regeneration of damaged CSTs was observed, and the regenerated fiber tracts descended along the posterior portion of the infarct (Fig 6). Four of these patients recovered from motor impairment, and one patient had partial motor dysfunction after 6 months. In three of eight patients, DT tractographic images showed that transpontine connective fibers that originated from the unaffected CST extended to the edge of the infarct and descended along the CST pathway (Fig 7). Motor function of the affected extremities slowly recovered to a near normal state in two patients. Slight motor dysfunction continued in the remaining patient.

Discussion

In the present study, we found that FA values of the CST distal to the pontine

Figure 5: Graph shows changes in FM scores with time in patients classified as having grade 1–3 CST involvement.

Figure 6: DT tractographic images superimposed on transverse diffusion-weighted *(A)* and T2-weighted *(B)* MR images in patient no. 7, a 56-year-old man with an acute infarct in the right pons (FM score, 50.0; Barthel index, 65; and modified Rankin scale score, 3 at the first examination and FM score, 78.0; Barthel index, 100; and modified Rankin scale score, 0 at the last examination). *A,* Images obtained on day 3 after onset show that most of CST of affected side passed through infarct (arrow). *B,* Images obtained on day 180 after onset show that some damaged fibers regenerated, reorganized, and descended along posterior portion of infarct (arrow).

infarct began to decrease within 1 week after onset. This progressive reduction in FA may be explained as myelinolysis and impaired structural integrity of the white matter due to Wallerian degeneration. FA values gradually returned to normal at various regions above the pons, which may be explained as glial cell proliferation, degradation of myelin, and removal of axonal debris. We also found that the subsequent degeneration in the CST after a pontine infarction may have slowed the process of neurologic recovery (especially motor function recovery), which may be

particularly useful for predicting the long-term recovery of motor function and facilitating clinical decision making.

The decrease in the FA value along the CST in the present study was relatively small, and the FA gradually increased as the disease progressed. In comparison with our results, those of previous studies (14,15) showed that FA values remained lower than those of the contralateral side even 1 year after infarction. It has been widely accepted that Wallerian degeneration is associated with the size and location of the infarct (16,17). Small lesions cause
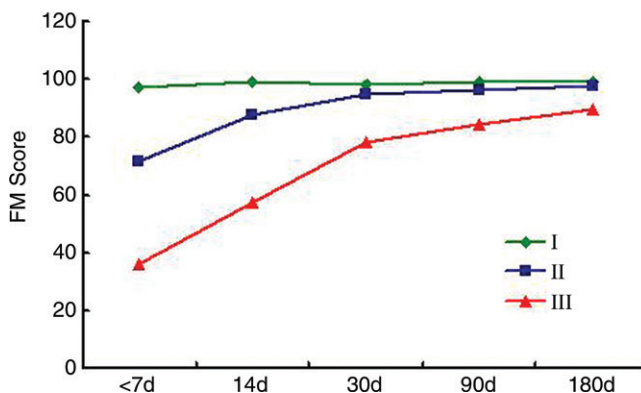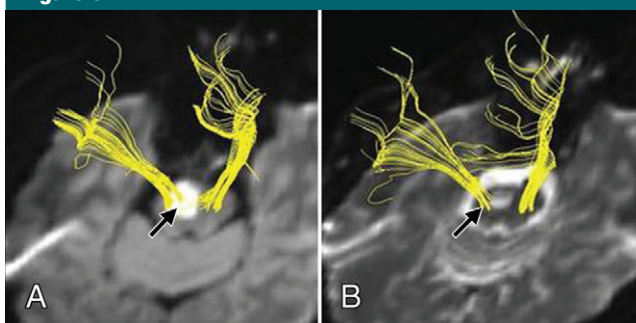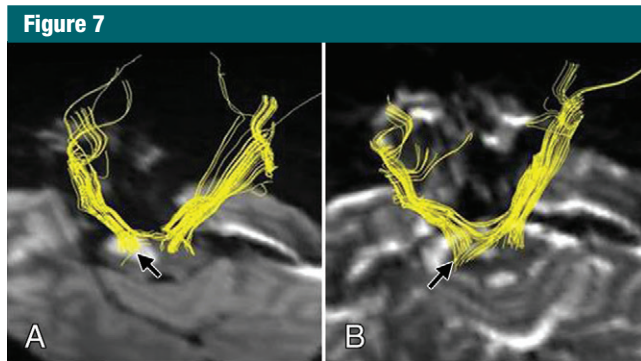
Figure 7

Figure 7: DT tractographic images superimposed on transverse diffusion-weighted MR images in patient no. 5, a 60-year-old man with an acute infarct in the right pons (FM score, 6.1; Barthel index, 20; and modified Rankin scale score, 5 at the first examination; FM score, 95.5; Barthel index, 100; and modified Rankin scale score, 0 at the last examination). *A,* Images obtained on day 3 after onset show that almost all of CST of affected side passed through infarct (arrow). *B,* Images obtained on day 180 after onset show transpontine connection fibers that originated from unaffected CST extended to edge of infarct (arrow).

only mild nerve fiber damage and are less likely to cause Wallerian degeneration. In addition, lesions involving the prefrontal cortex, parietal cortex, and corona radiata are most likely to cause Wallerian degeneration, followed by those at the basal ganglia and temporal lobe. Authors of most previous reports have focused on middle cerebral artery infarctions. In the current study, all patients experienced a unilateral pontine infarction, and even the largest lesion did not exceed the midline of the pons. Thus, the size, location, and CST involvement of the infarcts were different from those in previous reports. In addition, the regeneration and repair of the impaired nerve fibers could have slowed or terminated Wallerian degeneration.

DT tractography can display the spatial relationship between infarcts and the CST and also can be used to predict motor function outcomes (18–22). In our study, we found that the involvement of the CST was associated with the recovery of motor function by day 90 after onset. However, long-term follow-up on day 180 showed no such association, which indicates that motor function may be recovered in some patients with severe CST damage. Functional neuroimaging–based research (23–26) showed that early functional recovery after infarction was mainly related to the improvement of ischemia and edema around the lesion, whereas functional restoration at the chronic stages is closely related to the reorganization of brain function. We found evidence of multiple instances of structural remodeling and motor pathway compensation after pontine infarction. These data have important implications for the motor-recovery mechanism and rehabilitation of patients with a pontine infarct.

In the present study, during the recovery of motor function in some patients with severe CST damage, a few fibers arising from the contralateral CST crossed over to the ipsilateral side and down the edge of the infarct. Some of these fibers were along the conventional anatomic route of the CST, while others merged into the pontocerebellar fibers. Previous functional MR imaging studies have shown that, as an associated fiber in the cerebral-cerebellar circuitry, the pontocerebellar fiber is particularly important for motor function (27). In the present study, by using DT tractography, we found that the pontocerebellar fibers were important to the restoration of motor function. However, although the impaired CST showed evidence of regeneration and remodeling, this compensatory effect was very limited. Therefore, patients with more

CST involvement tended to have poorer prognoses.

There were a few potential limitations to our study. First, the DT imaging data acquisition time was relatively long, which was limiting for patients who found it difficult to remain still, and this may have resulted in the appearance of mild clinical symptoms in our patient group. Second, for various reasons, some patients could not be followed up, which led to the small sample size. Third, the signal-to-noise ratio of the original DT imaging examination may have influenced the fiber-tracking data, because a poor-quality original image could have reduced the reliability of fiber tracking (28,29). In future studies, a combination of DT imaging and functional MR imaging will be necessary to further elucidate the mechanisms of neural function rehabilitation. Development of more sophisticated DT tractographic postprocessing techniques and longitudinal study throughout a longer time frame is also important.

In summary, we found that decreased FA values along the CST in the early stages after pontine infarction could help predict the long-term outcome of motor dysfunction and that DT tractography could display the reorganization and regeneration of the motor pathways during the recovery process. These results will be useful in furthering our understanding of the motor recovery mechanism in patients with pontine infarct.

References

1. Carey LM, Seitz RJ. Functional neuroimaging in stroke recovery and neurorehabilitation: conceptual issues and perspectives. Int J Stroke 2007;2(4):245–264.

2. Fridman EA, Hanakawa T, Chung M, Hummel F, Leiguarda RC, Cohen LG. Reorgani-

zation of the human ipsilesional premotor cortex after stroke. Brain 2004;127(Pt 4): 747–758.

3. Jang SH. The role of the corticospinal tract in motor recovery in patients with a stroke: a review. NeuroRehabilitation 2009;24(3): 285–290.

4. Seitz RJ, Buetefisch CM. Recovery from ischemic stroke: a translational research perspective for neurology. Future Neurol 2006;1(5):571–586.

5. Assaf Y, Pasternak O. Diffusion tensor imaging (DTI)-based white matter mapping in brain research: a review. J Mol Neurosci 2008;34(1):51–61.

6. Neil JJ. Diffusion imaging concepts for clinicians. J Magn Reson Imaging 2008;27(1):1–7.

7. Cho SH, Kim DG, Kim DS, Kim YH, Lee CH, Jang SH. Motor outcome according to the integrity of the corticospinal tract determined by diffusion tensor tractography in the early stage of corona radiata infarct. Neurosci Lett 2007;426(2):123-127.

8. Yeo SS, Jang SH. Ipsilateral motor pathway without contralateral motor pathway in a stroke patient. NeuroRehabilitation 2012;30(4):303-306.

9. Kwon YH, Jeoung YJ, Lee J, et al. Predictability of motor outcome according to the time of diffusion tensor imaging in patients with cerebral infarct. Neuroradiology 2012;54(7): 691–697.

10. Lindenberg R, Renga V, Zhu LL, Betzler F, Alsop D, Schlaug G. Structural integrity of corticospinal motor fibers predicts motor impairment in chronic stroke. Neurology 2010;74(4):280–287.

11. Kim EH, Lee J, Jang SH. Motor outcome prediction using diffusion tensor tractography of the corticospinal tract in large middle cerebral artery territory infarct. NeuroRehabilitation 2013;32(3):583–590.

12. Liang Z, Zeng J, Zhang C, et al. Progression of pathological changes in the middle cerebellar peduncle by diffusion tensor imaging correlates with lesser motor gains after pontine infarction. Neurorehabil Neural Repair 2009;23(7):692–698.

13. Park JW, Kim SH, Kim YW, et al. Motor control via spared peri-infarct corticospinal tract in patients with pontine infarct. J Comput Assist Tomogr 2008;32(1):159–162.

14. Thomalla G, Glauche V, Weiller C, Röther J. Time course of wallerian degeneration after ischaemic stroke revealed by diffusion tensor imaging. J Neurol Neurosurg Psychiatry 2005;76(2):266–268.

15. Yu C, Zhu C, Zhang Y, et al. A longitudinal diffusion tensor imaging study on Wallerian degeneration of corticospinal tract after motor pathway stroke. Neuroimage 2009;47(2):451–458.

16. Kuhn MJ, Mikulis DJ, Ayoub DM, Kosofsky BE, Davis KR, Taveras JM. Wallerian degeneration after cerebral infarction: evaluation with sequential MR imaging. Radiology 1989;172(1):179–182.

17. Rabin BM, Hebel DJ, Salamon-Murayama N, Russell EJ. Distal neuronal degeneration caused by intracranial lesions. AJR Am J Roentgenol 1998;171(1):95–102.

18. Møller M, Frandsen J, Andersen G, Gjedde A, Vestergaard-Poulsen P, Østergaard L. Dynamic changes in corticospinal tracts after stroke detected by fibretracking. J Neurol Neurosurg Psychiatry 2007;78(6):587–592.

19. Kunimatsu A, Aoki S, Masutani Y, Abe O, Mori H, Ohtomo K. Three-dimensional white matter tractography by diffusion tensor imaging in ischaemic stroke involving the corticospinal tract. Neuroradiology 2003;45(8):532–535.

20. Lee JS, Han MK, Kim SH, Kwon OK, Kim JH. Fiber tracking by diffusion tensor imaging in corticospinal tract stroke: topographical correlation with clinical symptoms. Neuroimage 2005;26(3):771–776.

21. Konishi J, Yamada K, Kizu O, et al. MR tractography for the evaluation of functional recovery from lenticulostrate infarcts. Neurology 2005;64(1):108–113.

22. Hong JH, Lee J, Cho YW, et al. Limb apraxia in a patient with cerebral infarct: diffusion tensor tractography study. NeuroRehabilitation 2012;30(4):255–259.

23. Calautti C, Baron JC. Functional neuroimaging studies of motor recovery after stroke in adults: a review. Stroke 2003;34(6):1553–1566.

24. Pineiro R, Pendlebury S, Johansen-Berg H, Matthews PM. Functional MRI detects posterior shifts in primary sensorimotor cortex activation after stroke: evidence of local adaptive reorganization? Stroke 2001;32(5): 1134–1139.

25. Jaillard A, Martin CD, Garambois K, Lebas JF, Hommel M. Vicarious function within the human primary motor cortex? a longitudinal fMRI stroke study. Brain 2005;128(Pt 5):1122–1138.

26. Lazaridou A, Astrakas L, Mintzopoulos D, et al. fMRI as a molecular imaging procedure for the functional reorganization of motor systems in chronic stroke. Mol Med Rep 2013;8(3):775–779.

27. Lu J, Liu H, Zhang M, et al. Focal pontine lesions provide evidence that intrinsic functional connectivity reflects polysynaptic anatomical pathways. J Neurosci 2011;31(42): 15065–15071.

28. Chou MC, Lin YR, Huang TY, et al. FLAIR diffusion-tensor MR tractography: comparison of fiber tracking with conventional imaging. AJNR Am J Neuroradiol 2005;26(3): 591–597.

29. Batchelor PG, Atkinson D, Hill DL, Calamante F, Connelly A. Anisotropic noise propagation in diffusion tensor MRI sampling schemes. Magn Reson Med 2003;49(6): 1143–1151.